Journal of Colloid and Interface Science 680 (2025) 98–106

Contents lists available at ScienceDirect

Journal of Colloid And Interface Science

journal homepage: www.elsevier.com/locate/jcis

Regular Article

# A novel application of inverse gas chromatography for estimating contact angles in porous media

Mohammad Hossein Khoeini [a,*], Tomislav Vukovic [b,c], Antje van der Net [b,c], Azahara Luna-Triguero [a,d], Maja Rücker [a,d,e,*]

[a] Eindhoven University of Technology, Department of Mechanical Engineering, the Netherlands
[b] Norwegian University of Science and Technology, Norway
[c] Porelab Institute, Norway
[d] Eindhoven Institute for Renewable Energy Systems, the Netherlands
[e] Max Planck Institute for Polymer Research, Germany

## GRAPHICAL ABSTRACT

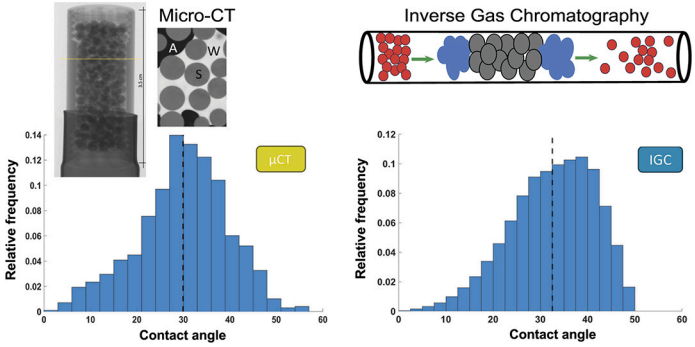


## ARTICLE INFO

*Keywords:*
Contact angle
Porous media
Multiphase flow
Inverse gas chromatography
Micro-CT
Wettability
Surface energy

## ABSTRACT

*Hypothesis:* Surface wettability is a critical factor in multi-phase flow within porous media, a processes essential in various applications e.g. in the energy sector. Traditional methods for assessing wettability of porous media by contact angle measurements, such as sessile droplet and micro-CT techniques, are limited by interface pinning, sample size or resolution impacting precision and accuracy. We hypothesized that using smaller and unconstrained probes, specifically gas molecules, to retrieve interactions along a representative sample size via inverse gas chromatography (IGC) could provide a more accurate determination of contact angles.

*Method:* We propose a procedure to relate IGC results with macro-scale wettability descriptions, such as the Young equation. To test the effectiveness of IGC method, glass bead samples with varying wettability, modified through a silanization process, were prepared. Contact angles for a distilled water-air-sample system were measured using the sessile droplet method and micro-CT for comparative analysis. IGC was employed to determine the surface energy components of these samples, which were then used in the extended Young-Dupré equation to calculate the contact angles.

*Findings:* The contact angle ranges determined by IGC and micro-CT for untreated glass beads, the most hydrophilic samples, showed great alignment. This consistency is attributed to the chemical amorphous nature of the untreated beads reflected in the assumption that dispersive and specific energetic components of surface

* Corresponding authors.
*E-mail addresses:* m.h.khoeini@tue.nl (M.H. Khoeini), m.rucker@tue.nl (M. Rücker).

https://doi.org/10.1016/j.jcis.2024.10.164
Received 2 September 2024; Received in revised form 21 October 2024; Accepted 25 October 2024
Available online 29 October 2024

sites are uncorrelated, on which the proposed analysis is based. For treated samples, where the silanization process creates correlations between surface energetic components, the alignment between IGC and micro-CT results was less precise. This study successfully demonstrated that IGC, a molecular-scale probe-based technique, can effectively determine the contact angle range, a macroscopic property, for amorphous samples. Future work should incorporate correlations between energetic components of surface detected by IGC to extend this method's applicability to a wider material range.

## 1. Introduction

Multiphase flow and reactive transport in porous media play a central role in many processes that are critical to the energy transition, such as subsurface carbon dioxide and hydrogen storage, and efficient fuel cells [1–3]. These phenomena are strongly affected by the porous medium's wettability, which describes the relative tendency of a solid to be in contact with one fluid over another [4]. Fluid displacement patterns in porous media, along with other factors such as the ratio of fluid viscosities, capillary number, and geometry of void space, are also strongly influenced by capillary forces, which are governed by the medium's wettability [4–7]. In reactive flow scenarios, the preferential affinity of the solid phase for one fluid can alter the reactivity of the porous media by covering active sites for the reactant fluid. This is exemplified by the adhesion of bubbles on electrodes during water electrolysis, which hinders the liquid phase's access to the electrodes, leading to a significant ohmic voltage drop and reduced process efficiency [8]. Therefore, accurately determining the wettability of porous media is essential for developing new materials and accurately predicting multi-phase and reactive flow in porous media.

The wettability of porous media is typically quantified on a local scale by the contact angle measured at the three-phase contact line [9]. Techniques commonly used for determining contact angles, such as sessile droplet and micro X-Ray computed tomography (micro-CT), have been shown to produce considerable variability in measured values at thermodynamic equilibrium for the same materials [10–13]. A primary factor contributing to this variability is the inherent resolution limitation of these imaging-based techniques, which hinders their ability to accurately and precisely identify the contact line at the three-phase contact point. This challenge is particularly pronounced when the surface roughness features are below the resolution threshold of the techniques used [14–18].

Furthermore, the surface of porous media, which frequently exhibits roughness from the nano-scale upwards, is often composed of various chemical constituents and/or contains impurities, resulting in a range of contact angles across the porous medium's surface [4,19]. The aforementioned techniques are limited to determining the contact angle at specific locations where the fluids' interfaces are located. Hence, the measured values solely reflect a fraction of surface and fail to capture the overall surface wettability.

To address the resolution and localized measurements, employing smaller and unconstrained probes, such as gas molecules, can be beneficial. Inverse gas chromatography (IGC), a well-established technique, exploits gas probes to characterize the physiochemical properties of porous material. This method involves injecting various concentrations of different gas probes into a column packed with the porous media under investigation. The intensity and extent of interactions between probes and porous media, measured at the column's outlet, are used for determining surface properties of the solid, such as surface energy [20–22]. Notably, in addition to the surface tension of fluids, surface energy of the solid is a key parameter that correlates the contact angle with wettability, as described by the Young equation [10]. Another advantage of this technique is its capability to precisely control the amount of gas probes injected into the column [21]. The use of small concentration of gas probes, known as infinite dilution or zero coverage condition, enables the selective analysis of high energy sites [23], which are potential pinning points of contact angles [24,25]. By increasing the concentration of injected probe molecules, the evaluation can be extended to lower-energy sites, until the probe-probe interactions overshadow the probe-solid interactions. Through these controlled variations in probe concentrations, this methodology thereby allows determining the energy heterogeneity of porous media [26,27].

IGC has been previously utilized alongside other surface characterization techniques, such as sessile droplet, in numerous studies [28–35] to assess the wettability of porous media and determine surface energy values. However, its application has primarily been limited to comparing surface energy values derived under the infinite dilution mode of IGC, using very small concentrations of gas probe, with those obtained from other methodologies. The potential of IGC to measure the energy heterogeneity of porous media, which can then be utilized to calculate a range of contact angles using known fluids surface tensions and theoretical frameworks such as the Young equation, remains unexplored, to the best of the authors' knowledge. A major advantage of IGC method is its ability to assess surface energy heterogeneity of porous media without dependency on the fluids types, thereby enabling the prediction of contact angle ranges for any fluids-porous medium combination.

In this study, we aim to evaluate the feasibility of directly determining contact angles from IGC measurements. Glass beads are selected as test samples due to their common use in studies of multiphase flow in porous media [11]. To minimize the complexities and variability associated with the internal porosity of typical porous materials, non-porous glass beads are selected to enable a more accurate evaluation of the IGC method's performance. Furthermore, to assess the method's performance across a range of wettabilities, the glass beads, which are standardly hydrophilic, are treated with a silanization process to induce varying levels of hydrophobicity. For a comprehensive evaluation of the new method's performance, the contact angles derived from IGC measurements will be compared with values obtained using micro-CT and the sessile droplet techniques. The use of non-porous glass beads, which form a macro-porous structure when packed, mitigates the additional complexities that porous materials introduce during the interpretation of micro-CT data [36,37]. This approach facilitates a more straightforward and reliable comparison between the micro-CT and IGC-based methods.

## 2. Methodology

### 2.1. Sample preparation

In this study, samples were prepared according to the procedure outlined in [11]. Non-porous soda lime glass beads, with average diameters of 1 mm and 2 mm, purchased from Karl Hecht Assistent, were first cleaned using a sequential rinsing procedure with toluene, methanol, and acetone, all sourced from VWR Chemicals. Each solvent rinse lasted at least 30 seconds. The composition of the cleaned glass beads was assessed using electron probe microanalysis, which confirmed that the beads can be characterized as soda lime glass. The exact composition values are detailed in [11].

Following the cleaning process, two reference sample packs were left untreated, while two additional packs were treated with different concentrations of Surfasil, a silanizing reagent, purchased from Thermo Scientific. Specifically, these packs were treated with 0.001 and 0.01 volume ratios (VR) of Surfasil to n-heptane (solvent) mixtures at room temperature. The glass beads were submerged in these solutions for 180

seconds using a sieve, which was then used to remove them from the solutions. To stop the silanization reaction and prevent further interaction with water, the beads were immediately rinsed with pure n-heptane followed by methanol. Finally, the treated samples were placed in an oven at 80 °C for 2 hours to evaporate the solvents.

### 2.2. Inverse gas chromatography

#### 2.2.1. Basic theoretical aspects of IGC

IGC is a gas-solid analytical technique widely utilized to determine the physicochemical properties of solids, fibers, and films [20,22]. One of its most common applications is measuring the surface free energy of solids. Regarding the principles of IGC measurements, the primary data obtained from this technique is the retention time. The retention time is defined as the time required for a specific quantity of probe molecules to elute through a packed column containing the sample under investigation. This time reflects the strength of the interaction between the probe and the surface. To account for factors influencing retention time, such as flow rate and temperature, the net retention volume is derived from the retention time using:

$$V_n = \frac{j}{m}.F.(t_R - t_0).\frac{T}{273.15} \quad (1)$$

where $T$ is the column temperature in Kelvin (K), $F$ is the carrier gas flow rate leaving the column ($mL/min$), $m$ is the mass of the sample in the packed column, $j$ is the James–Martin correction factor (which adjusts for pressure drop along the column), $t_R$ is the retention time of the injected probe, and $t_0$ (or dead time) is the time required for probe molecules to pass through the column without interaction, typically measured by injecting methane. The net retention volume can then be related to the standard molar Gibbs free energy change associated with the isothermal sorption of the probe ($\Delta G^0$), and the work of adhesion of the probe to the surface ($W_A$), as given by [38,39]:

$$\Delta G^0_{des} = -\Delta G^0_{ads} = RT\ ln(V_n) + C = N_A.a_m.W_A \quad (2)$$

Where $N_A$ is the Avogadro number, $a_m$ is the cross-section area of the single adsorbed molecule of the probe, $R$ is the gas constant, and $C$ is a constant dependent on the chosen reference state [38]. The Gibbs free energy of sorption can be described as the sum of the contributions from both dispersive (D) and specific interactions (SP) between the probe and the surface, as shown below:

$$\Delta G^t_{ad} = \Delta G^D_{ad} + \Delta G^{SP}_{ad} \quad (3)$$

The work of adhesion between the probe and the solid surface can be expressed in terms of the surface energy components of each phase using the approach developed by Van Oss et al. [40]:

$$W_A = 2.(\sqrt{(\gamma^d_P.\gamma^d_S)} + \sqrt{(\gamma^+_P.\gamma^-_S)} + \sqrt{(\gamma^-_P.\gamma^+_S)}) \quad (4)$$

Where $\gamma_P$ and $\gamma_S$ denote the surface energy of the probe and solid, respectively, and the superscripts d, +, and - represent the dispersive component, electron-donor, and electron-acceptor parameters of the specific component of surface energy. Owens and Wendt [41] proposed a shortened form of Eq. (4), in which the electron-donor and electron-acceptor parameters are combined into a single specific component ($\gamma^{SP}_P$), as follows:

$$W_A = 2.(\sqrt{(\gamma^d_P.\gamma^d_S)} + \sqrt{(\gamma^{SP}_P.\gamma^{SP}_S)}) \quad \text{where} \quad \gamma^{SP}_S = \sqrt{\gamma^-_S.\gamma^+_S} \quad (5)$$

***Dispersive component of surface energy:*** The dispersive component of surface energy ($\gamma^d_S$) can be assessed using non-polar probes, which interact solely via dispersive forces with the surface (with $\gamma^+_P = \gamma^-_P = 0$). Schultz et al. [38] demonstrated that by injecting a series of n-alkanes and plotting $RT\ln(V_n)$ versus $N_A.a_m.(\gamma^d_P)^{0.5}$, the dispersive component of surface energy can be derived from the slope of the resulting linear relationship, as shown in Fig. 1.

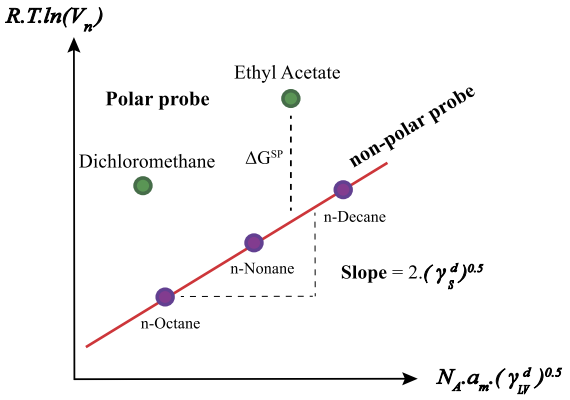


**Fig. 1.** Schematic representation of the determination of dispersive component of surface energy ($\gamma^D_S$) by Schultz method.

***Specific components of surface energy:*** The specific component of surface energy can be quantified using polar probe ($\gamma^{SP}_P \neq 0$). In this case, the total work of adhesion encompasses both dispersive and specific interactions [42,43]. Knowing the cross section area ($a_m$) and dispersive component of surface tension ($\gamma^D_P$) of polar probe enables the calculation of specific component of surface energy of solid using Equations (2) and (5). To exclusively determining the electron-donor or electron-acceptor of surface (often referred to in literature as acidity and basicity, respectively), mono-polar probes, where either $\gamma^-_P = 0$ or $\gamma^+_P = 0$, can be employed as polar probes (using Equations (2) and (4). In this approach, it is assumed that the dispersive components of surface sites, as used in these equations, are consistent with those calculated from interactions of dispersive probes (n-alkanes) with the surface. This assumption implies that polar probes interact with the same surface sites as those probed by dispersive probes.

***Surface energy distribution:*** As previously discussed, injected probe molecules initially interact with the highest energetically accessible sites on the surface. Once these high-energy sites are occupied, subsequent probe molecules interact with lower-energy sites [44,45]. Thus, the retention time of injected probe molecules provides an average measure of the injected probe molecules interactions with these various sites [46]. By increasing the concentration of injected probe molecules, one can extend the analysis of surface energy components from focusing solely on the highest-energy sites to averaging across a broader spectrum of energetic sites, from highest to lower-energy sites. However, as the number of injected probe molecules increases, interactions between additional probe molecules and lower-energy sites can become comparable to probe-probe interactions. At this stage, the adsorption process may enter a multilayer regime, where probe-probe interactions start to affect the retention time, thereby potentially compromising the accuracy of surface energy determination based on retention time. As a result, this method may not effectively characterize the surface sites with energy levels lower than the surface tension of the probes used in the IGC measurements.

Thielmann et al. [23,47] developed a methodology for quantifying surface energy heterogeneity by employing varying concentrations of probes. This technique involves multiple injections with progressively increasing concentrations of both dispersive (n-alkanes) and polar probes. Following these injections, the retention volume of each probe is correlated with the corresponding surface coverage, which indicates the proportion of the surface area occupied by the adsorbed probes.[1] Once the relationship between retention time and surface coverage is established, the dispersive and specific components of surface energy can be

[1] For detailed steps on calculating surface coverage and other methodological specifics, please refer to the main article [47].

calculated for each level of surface coverage. It is important to note that the developed methodology relies on the same underlying assumption for determining specific surface energy as outlined in section 2.2.1. Specifically, it assumes that polar probes interact with the same surface sites as those probed by dispersive probes. When this assumption is extended to increasing concentrations of probes, it implies that polar probes interact with the same surface sites in the same sequence, ranging from highest to lowest energy levels, as dispersive probes.

#### 2.2.2. Experimental procedure using IGC

IGC measurements on the untreated and two treated samples, 0.001 VR and 0.01 VR (as described in section 2.1, were conducted using the IGC-SEA system from Surface Measurement Systems Ltd., London, UK. The glass bead samples (1 mm) were packed into silanized standard columns with dimensions of 3 mm inner diameter and 30 cm length, and were secured using silanized glass wool. Prior to measurement, the columns were conditioned for 3 hours at 60 °C to purge any physisorbed impurities. All IGC injections were performed at 30 °C with a flow rate of 10 $mL/min$. Methane and nitrogen were employed as non-interacting probe, for determination of the column dead time, and as carrier gas, respectively.

The dispersive component of the samples' surface energy at each surface coverage was quantified using a series of n-alkanes (n-octane, n-nonane, n-decane). The basic and acidic parameters of the samples' surface energy were assessed using ethyl acetate and dichloromethane as monopolar probes, respectively. These parameters were subsequently used to calculate the specific component of surface energy using Equation (5). All chemicals were of HPLC grade and sourced from Sigma-Aldrich. The retention time for each injection was determined from the center of mass of the corresponding chromatographic peak. To investigate potential procedural errors, three replicate columns of untreated glass bead samples were prepared.

### 2.3. Micro-CT and Sessile droplet reference data

The experimental procedures and results for contact angle measurements using the Sessile droplet and micro-CT techniques have been comprehensively detailed in a prior publication [11]. It should be noted that the selected sample size allowed for direct contact angle measurements using these techniques without acquiring higher resolution imaging or requiring additional processing steps. Such processing, like compacting or adhering, is typically required to enable contact angle measurements for smaller sample sizes, e.g. for powders [48]. However, these steps can alter the inherent surface properties of the sample, thereby compromising the accuracy and reliability of comparisons with the IGC data.

*Contact angle measurement using the sessile droplet technique* Contact angle measurements for the distilled water-air-glass bead system were conducted using a Kruss DSA100S drop shape analyzer at ambient temperature (23 °C). This apparatus comprises a high-intensity monochromatic LED light source, a camera with a resolution of μm, and a software-controlled syringe system capable of dispensing liquid with a precision of 0.1 μL.

The procedure for measuring contact angles was as follows: A droplet of distilled water was first deposited onto a glass plate. A glass bead, with a diameter of 2 mm, was then carefully positioned in the center of the droplet using tweezers. The camera system captured high-resolution images of the bead in the water droplet throughout the evaporation process. Imaging continued until the water had fully evaporated, leaving only the glass bead on the glass plate.

Post-processing of the images was performed using ImageJ software. To determine the contact angle, the final image, which depicted the bead remaining on the dry surface, was overlaid with the initial image taken when the bead was in the water droplet. This image overlay allowed for the identification of the three-phase contact line and enabled the measurement of the contact angle.

*Contact angle measurement using the micro-CT technique* To determine the contact angles using the micro-CT technique, 2 mm glass beads were packed into a cylindrical container with dimensions of 3.5 cm in height and 1.4 cm in diameter. The beads were secured within the container using screw-on caps at both ends. Prior to introducing the distilled water, a dry scan of the packed beads was conducted to create a baseline image for use in segmentation during image processing.

Distilled water, enhanced with 1.4 M cesium chloride (CsCl) for contrast, was then gently injected into the container from the top using a syringe. To ensure that equilibrium contact angles were accurately captured, the sample was rotated in the scanner beforehand to minimize movement of the interfaces and beads during scanning. This rotation was applied for approximately 18 minutes, matching the duration of the final scan.

The sample was scanned using a Nikon XT H 225 CT scanner with the following parameters: an imaging resolution of 12 μm, a source voltage of 160 $kV$, a source current of 75 μA, and an exposure time of 117 ms. Image segmentation was performed using ORS Dragonfly software, applying pixel thresholding based on the method proposed by Otsu [49]. This method facilitated the identification of the three phases (water, air, and solid) in the segmented images. Contact angles were subsequently measured from the segmented images following the approach detailed by AlRatrout et al. [50]. Further details on image processing and results are available in [11].

## 3. Theoretical basis for contact angle calculations from surface energy distributions measured with IGC

### 3.1. From Young Equation to the characterization of solid surface energies

The wettability involves three interfaces from three media interacting along a single line of contact. The balance among these interfaces and the position of the contact line are governed by the surface energetics of the system. Over 200 years ago, Thomas Young provided a quantitative framework for describing the energetic balance between interfaces. The Young's Equation relates the equilibrium contact angle to the interfacial free energies of the liquid-solid ($\gamma_{LS}$) interface, the surface energy of solid-vapor ($\gamma_{SV}$), and the surface tension of liquid-vapor ($\gamma_{LV}$):

$$\gamma_{SV} = \gamma_{LV}.cos\Theta + \gamma_{SL} \tag{6}$$

Here, surface free energy (or surface tension) represents the attractive intermolecular forces between the surface molecules of different phases at the interface [43]. In principle, the interactions between phases arise from the excess energy of surface molecules compared to those in the bulk, which drives the surface molecules to interact with other phases to achieve energetic compensation. The total surface free energy of a material comprises several types of physical forces, which can be categorized into distinct components. Materials always interact through Lifshitz van der Waals, and depending on the availability of corresponding sites on the surface, may also interact through other forces such as hydrogen-bonding, acid-base interactions. Consequently, surface free energy is often divided into two main components: the dispersive component ($\gamma_s^d$), which accounts for Lifshitz van der Waals forces, and the specific component ($\gamma_s^{SP}$), which includes all other types of intermolecular interactions:

$$\gamma_{SV}^t = \gamma_{SV}^d + \gamma_{SV}^{SP} \tag{7}$$

To connect the theoretical description of surface free energy components with practical measurements, such as contact angle, the Owens, Wendt, Rabel, and Kaelble model (OWRK) [41,51] provides a useful framework. It proposes that the interfacial free energy of the liquid-solid interface ($\gamma_{LS}$) can be represented as the sum of the geometric mean of the dispersive and specific components of the solid's surface

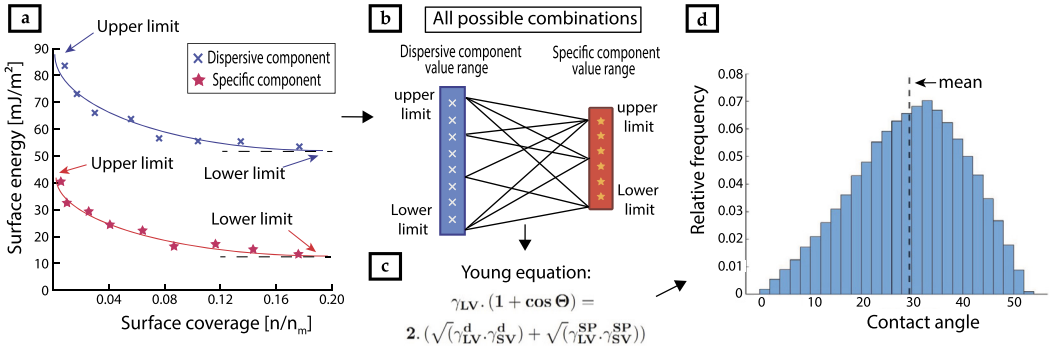


**Fig. 2.** Schematic diagram illustrating the determination of contact angle range from surface energy component profiles obtained via IGC. (For interpretation of the colors in the figure(s), the reader is referred to the web version of this article.)

energy. When combined with Young's Equation, this model leads to the following relationship [52]:

$$\gamma_{LV} \cdot (1 + cos\,\Theta) = 2 \cdot (\sqrt{(\gamma_{LV}^{d} \cdot \gamma_{SV}^{d})} + \sqrt{(\gamma_{LV}^{SP} \cdot \gamma_{SV}^{SP})}) \quad (8)$$

Van Oss et al. [40] further refined this approach by subdividing the specific component of surface energy into electron-acceptor ($\gamma^{+}$) and electron-donor ($\gamma^{-}$) components. This approach is based on the concept that the specific component of surface energy depends on the availability of sites capable of undergoing specific types of interactions. When integrated with Young's Equation, this approach provides a more detailed framework for understanding the interfacial free energy, as describe by:

$$\gamma_{LV} \cdot (1 + cos\,\Theta) = 2 \cdot (\sqrt{(\gamma_{LV}^{d} \cdot \gamma_{SV}^{d})} + \sqrt{(\gamma_{LV}^{+} \cdot \gamma_{SV}^{-})} + \sqrt{(\gamma_{LV}^{-} \cdot \gamma_{SV}^{+})}) \quad (9)$$

### 3.2. Contact angle determination from surface energy distribution

From a theoretical standpoint, assessing surface energy through vapor adsorption techniques such as IGC is conceptually equivalent to using liquid interaction methods like contact angle measurements [45]. Contact angle measurements are generally believed to reflect the mean surface energy of the sites covered by the liquid [32]. To accurately capture the wettability of the solid, contact angle measurements should ideally employ very small liquid droplets, typically in the range of 5-10 μm [17]. This small droplet size minimizes the impact of droplet size on the measurement, but it necessitates performing numerous measurements to achieve a comprehensive evaluation of the entire surface. Additionally, surface roughness and chemical heterogeneity may cause barriers to the motion of the contact line, resulting in variability in the measured contact angle and surface energy values.

In contrast, IGC offers advantages over these conventional liquid/optical methods by circumventing issues arising from surface roughness and morphology [32]. Moreover, the surface energy distribution obtained from IGC not only provides comparable and potentially more precise information than contact angle measurements but also offers insights into factors affecting contact angle measurements, such as the pinning effect. At low surface coverage, IGC reveals the surface energy of sites that are most likely to influence contact angle pinning. On the other hand, at high surface coverage, the surface energy value obtained should approximate the value derived from contact angle measurements. However, since probe molecules interact with the entire surface in IGC, this value should align with the average contact angle reported if measurements were conducted over the entire surface.

Furthermore, the surface energy components profiles obtained from IGC provide a range of values that any user-selected probing liquid would encounter when placed on different areas of the surface. In other words, the interaction between the liquid and the surface would be determined by these surface energy values, depending on the liquid's chemical nature. As a result, by applying different combinations of values from these profiles within appropriate theoretical frameworks, such as the modified Young equation for relatively smooth samples, it is possible to estimate the range of contact angles for any chosen liquid, provided its surface tension is known. In other terms, IGC quantifies the surface energy of solids, allowing for the determination of contact angles for various fluids without direct interaction between the fluid and the solid.

In this study, the upper and lower bounds of the surface energy range for each component were determined by fitting an exponential decay function to the experimental data (see Fig. 2.a). Subsequently, all possible combinations of surface energy values were derived by dividing the energy ranges of each surface energy component (Fig. 2.b). Since the glass beads are relatively smooth, the use of the modified Young equation, which is formulated based on surface energy components (equation (8)), is considered appropriate (Fig. 2.c). The dispersive and specific components of the surface tension of distilled water at 23 °C are 51.3, and 21.1 $mJ/m^2$, respectively [53,54]. By applying all combinations of surface energy components along with the surface tension components of distilled water (the probing liquid) in equation (8), a histogram of the contact angle range can be generated (Fig. 2.d).

## 4. Results and discussion

In this study, to assess the effectiveness of IGC in determining the contact angle range, we prepared three glass bead samples with varying wettability (as detailed in subsection 2.1). To provide a comparative analysis between IGC and other established methodologies, the contact angle for distilled water-air-sample system were determined using sessile droplet and micro-CT methods, as described in subsection 2.3, with results already reported in [11]. In the following subsections, we will first discuss the results for untreated glass beads and then present the findings for treated samples.

### 4.1. Match between surface energies and macroscopic contact angle distribution for untreated glass beads

The surface energy components and contact angle ranges determined by IGC from three separate replicate columns of untreated glass beads are shown in Fig. 3. The observed decreasing trend in the specific component of surface energy for the replicate samples falls within a margin of $\pm 2 mJ/m^2$. However, the larger variation for the dispersive component, at $\pm 4 mJ/m^2$, is observed. Despite potential influences such as human error, non-homogeneity in column packing, data acquisition and processing errors [21,55], and the relatively small surface area of the glass beads compared to typical materials used in IGC measurements [56], the error margins for both the dispersive and specific components are considered reasonable. The average contact angles for these replicated samples are 33.6°, 28.8°, and 27.7°, respectively. Although small variation in surface energy values can lead to notable variations in the contact angle according to the modified Young's equation, the contact

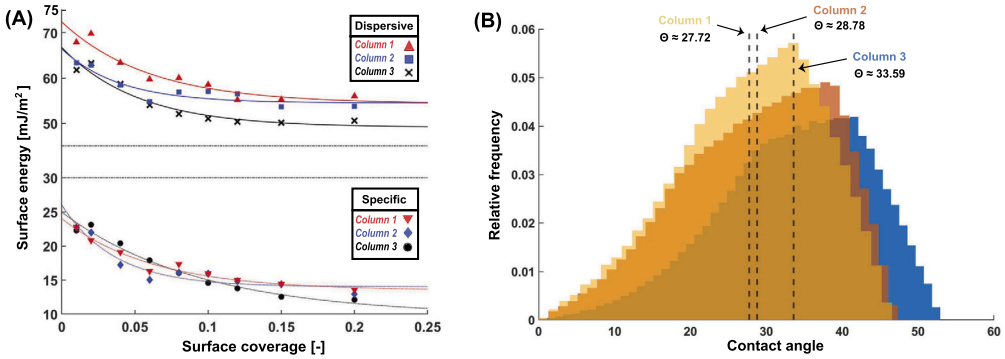


**Fig. 3.** Surface energy components for three replicate columns of untreated glass beads (Panel A) and the histogram of corresponding contact angle ranges derived from these values (Panel B).

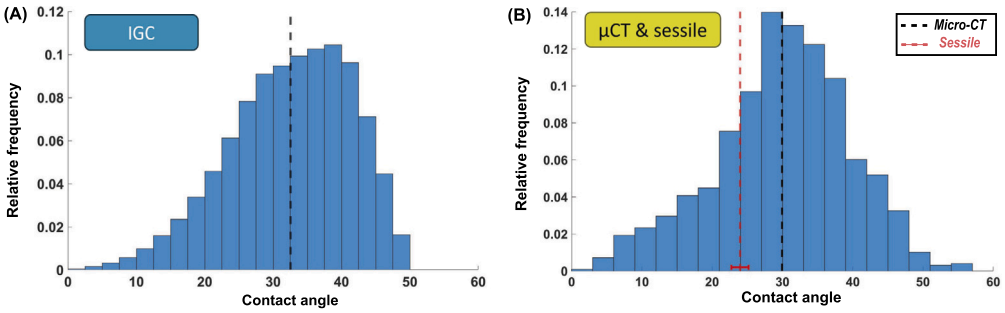


**Fig. 4.** Histograms illustrating the contact angle range for the distilled water-air-untreated glass bead system: Panel (A) shows contact angles derived from the average surface energy components of three replicate samples measured by IGC. Panel (B) presents contact angles obtained from micro-CT, with additional sessile droplet measurements shown as a line with error bars.

angle ranges obtained from the replicate columns remain within the within reasonable limits.

The sessile droplet method yielded an average contact angle of $23.95 \pm 1.25°$ for untreated glass bead sample. The contact angle ranges determined by IGC, based on the average surface energy components of three replicated samples, as well as by micro-CT and sessile droplet measurements, are shown in Fig. 4. The results from both IGC and micro-CT methods show remarkable alignment with contact angles ranging between 0° - 55° and a peak at 31.57° and 29.93°, respectively. Both methods exhibited non-Gaussian distributions, with a slight bias toward higher contact angles. The combination of average values and contact angle ranges offers a practical basis for comparing the methods.

The observed results were surprising given the anticipated limitations of each technique. Micro-CT was expected to lack necessary resolution to resolve detailed surface features. Furthermore, it only provides contact angle distributions along the three-phase contact line, rather than over the entire surface as IGC does. Conversely, IGC was presumed to not be capable of providing sufficient information to recover dynamic (advancing and receding) contact angle. The remarkable consistency between these techniques may be attributed to the specific characteristics of the chosen sample: the amorphous chemical nature and relatively smooth texture of the surface of untreated glass beads.

The smoothness of the beads supports the validity of applying the Young equation to calculate contact angles from surface energy components. Furthermore, the amorphous (non-crystalline and irregular) nature of the glass bead surface implies that no systematic relationship between the specific and dispersive components of surface energy at individual sites can be established. In such samples, a probabilistic model of molecular interactions based on IGC appears to effectively characterize the energy landscape of the surface, thereby allowing for precise determination of the contact angle range, including dynamic angles, using the developed method.

### 4.2. Monitoring wetting alteration using IGC for surfasil-treated glass beads

The IGC measurements on the two altered glass beads reveal a shift towards greater water repellency.[2] For the less modified sample (0.001 VR), contact angles ranged from 34.8° to 99.2°, with an average of 60.82°. The more modified sample (0.01 VR) exhibited a range of 49.3° to 100.8°, averaging 69.2°. These results are illustrated in Fig. 5 panels A and B, respectively. Similarly, the Sessile droplet method reported contact angles of $64.2 \pm 2.04°$ for 0.001 VR sample, and $88.9 \pm 2.48°$ for the 0.01 VR sample. These findings are consistent with the micro-CT measurements shown in Fig. 5 panels B and D, respectively, and confirm a significant alteration in the wettability of the treated glass beads.

However, the average contact angle range determined by micro-CT is 17.2° higher for the lesser modified sample and 25° higher for the more modified sample compared to the IGC measurements. Additionally, the range of contact angles from micro-CT is broader in both cases. Although micro-CT results may be influenced by pinning effects and resolution limitations, the smoothness of the glass beads is unlikely to have been significantly altered by the thin layer of silanizing agent. Consequently, the observed discrepancies between the contact angle ranges obtained from IGC and micro-CT are more plausibly attributed to the inadequacy of the assumptions underlying the IGC data analysis. Specifically, the silanizing agent introduces regions with non-specific energetic properties (solely dispersive), thereby challenging the IGC assumption that polar probes interact with the same sequence of surface sites as dispersive probes, as explained in subsubsection 2.2.1.

To address the limitations observed in IGC data analysis, one promising approach is to perform experiments at controlled relative humidity. Conditioning the IGC column at different humidity levels allows for

[2] The results of the surface energy components of treated samples are provided in the Appendix A.

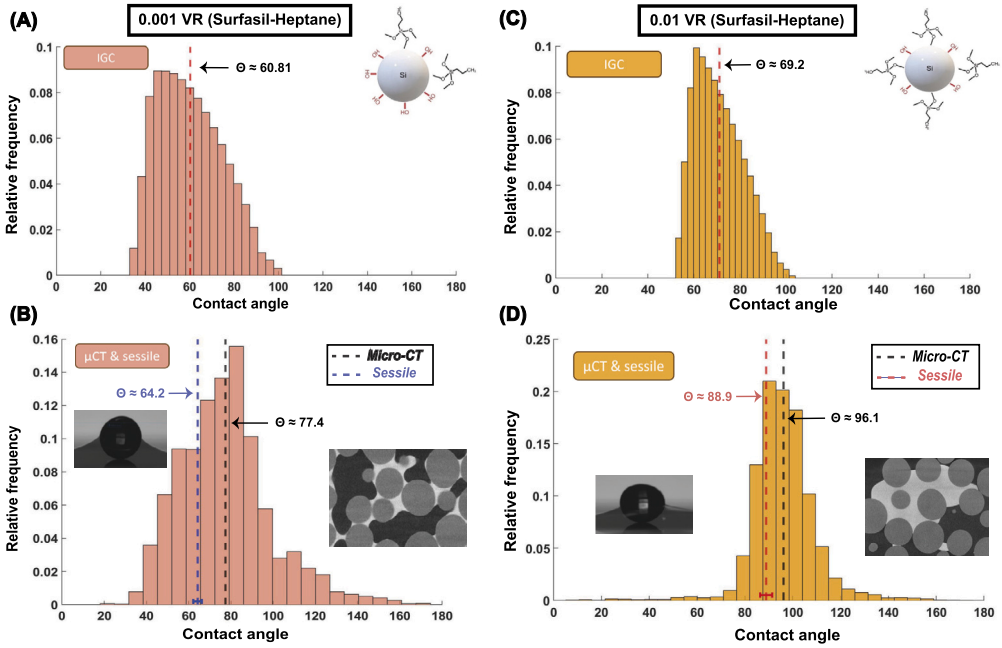


**Fig. 5.** Histograms depicting the contact angle range for the 0.001 VR treated sample, as determined by IGC (A) and micro-CT (B), and for the 0.01 VR treated sample, as determined by IGC (C) and micro-CT (D).

the progressive coverage of the surface's functional groups with water through condensation [57]. This method is advantageous because dispersive probes, such as n-alkanes, will primarily interact with the surface areas that are not covered by water [56]. By obtaining surface energy components at various relative humidity levels, it becomes possible to explore the correlations between different surface energy components more comprehensively. However, for this approach to be fully effective, future research must account for the competitive adsorption of polar probes with water, as well as the adsorption of polar probes onto the water-covered surface.

## 5. Conclusions

This study represents a pioneering effort in introducing a novel approach for directly determining contact angle ranges from IGC measurements. In contrast to previous studies [28–35], which primarily compared surface energy values obtained from contact angle measurements with those derived from IGC, our work is the first to utilize surface energy distributions obtained from IGC to calculate a range of contact angles through a newly developed approach. This methodology not only extends the application of IGC but also addresses the inherent limitations of image-based techniques such as micro-CT and sessile droplet methods, which are often constrained by issues of resolution and localized measurements.

To evaluate the effectiveness of the IGC method across a range of wettabilities, glass beads, which are commonly used in multiphase flow studies in porous media, were selected as test samples and modified through a silanization process. Non-porous glass beads were specifically chosen to avoid complications and additional variables that could arise from porosity, thereby providing a clearer assessment of the IGC method's performance and its comparison with other methods such as micro-CT and sessile droplet. The results indicate that IGC is a robust technique for characterizing wettability in porous media, as demonstrated by the strong correlation between the contact angle ranges derived from IGC and those determined by micro-CT measurements for unmodified glass beads, both in terms of average values and their distribution. This consistency supports the hypothesis that molecular interactions experienced by the probe molecules in porous media can be correlated with macroscopic wettability, validating the broader applicability of IGC in material characterization. This relationship is expected to impact applications relying on molecular modeling-based designed materials, particularly direct air capture [58], catalysis [59], and fuel cells [60]. A clear advantage of the versatility of IGC over micro-CT is its capability to analyze samples with more confined porosity over relevant sample sizes, making it particularly suitable for studying wettability in materials with specific pore structures.

For silanized glass beads, IGC effectively detected changes in wettability induced by the silanization process, although it exhibited a smaller shift toward increased hydrophobicity compared to micro-CT. This discrepancy underscores the limitations of IGC data interpretation, particularly in the context of chemically heterogeneous surfaces. Future research should focus on refining the IGC data analysis methodology, particularly in establishing a more accurate relationship between the specific and dispersive components of surface energy to better account for chemically heterogeneous surfaces. Additionally, further studies should explore the application of IGC to porous samples, as pore size can influence contact angle measurements. This will involve applying theories such as Wenzel or Cassie-Baxter to accurately describe macroscale contact angles and adapting IGC data analysis techniques to ensure that material porosity is adequately considered. These advancements will help extend the applicability and precision of IGC in characterizing wettability across a broader range of materials.

In conclusion, this study highlights the potential of IGC as a versatile tool for wettability assessment. However, continued refinement of this method will be essential for extending its applicability to more chemically complex and heterogeneous materials, as well as to porous samples where pore size can influence contact angle measurements. Addressing these aspects will improve the accuracy and reliability of wettability characterization across a diverse range of materials.

## CRediT authorship contribution statement

**Mohammad Hossein Khoeini:** Writing – original draft, Visualization, Validation, Software, Resources, Methodology, Investigation, Formal analysis, Conceptualization. **Tomislav Vukovic:** Resources, Investigation, Formal analysis. **Antje van der Net:** Writing – review & editing, Supervision, Funding acquisition. **Azahara Luna-Triguero:** Writing – review & editing, Supervision, Project administration. **Maja Rücker:**

Writing – original draft, Supervision, Project administration, Funding acquisition, Conceptualization.

## Declaration of competing interest

The authors declare that they have no known competing financial interests or personal relationships that could have appeared to influence the work reported in this paper.

## Acknowledgement

This research has received funding from the NWO DeepNL program (DEEP.NL.2019.006) and NWO (project 19121). The Research Council of Norway is acknowledged for its support through project 262644 (Pore-lab Center of Excellence). The authors also acknowledge Surface Measurement Systems for valuable discussions.

## Appendix A. Supplementary material

Supplementary material related to this article can be found online at https://doi.org/10.1016/j.jcis.2024.10.164.

## Data availability

Data will be made available on request.

## References

[1] N. Heinemann, J. Alcalde, J.M. Miocic, S.J.T. Hangx, J. Kallmeyer, C. Ostertag-Henning, A. Hassanpouryouzband, E.M. Thaysen, G.J. Strobel, C. Schmidt-Hattenberger, K. Edlmann, M. Wilkinson, M. Bentham, R. Stuart Haszeldine, R. Carbonell, A. Rudloff, Enabling large-scale hydrogen storage in porous media – the scientific challenges, Energy Environ. Sci. 14 (2) (2021) 853–864, https://doi.org/10.1039/D0EE03536J.

[2] R. Borup, J. Meyers, B. Pivovar, Y.S. Kim, R. Mukundan, N. Garland, D. Myers, M. Wilson, F. Garzon, D. Wood, P. Zelenay, K. More, K. Stroh, T. Zawodzinski, J. Boncella, J.E. McGrath, M. Inaba, K. Miyatake, M. Hori, K. Ota, Z. Ogumi, S. Miyata, A. Nishikata, Z. Siroma, Y. Uchimoto, K. Yasuda, K.-i. Kimijima, N. Iwashita, Scientific aspects of polymer electrolyte fuel cell durability and degradation, Chem. Rev. 107 (10) (2007) 3904–3951, https://doi.org/10.1021/cr050182l.

[3] K. Damen, A. Faaij, W. Turkenburg, Health, safety and environmental risks of underground Co2 storage – overview of mechanisms and current knowledge, Clim. Change 74 (1) (2006) 289–318, https://doi.org/10.1007/s10584-005-0425-9.

[4] A. Mascini, V. Cnudde, T. Bultreys, Event-based contact angle measurements inside porous media using time-resolved micro-computed tomography, J. Colloid Interface Sci. 572 (2020) 354–363, https://doi.org/10.1016/j.jcis.2020.03.099.

[5] S. Pavuluri, R. Holtzman, L. Kazeem, M. Mohammed, T.D. Seers, H.S. Rabbani, Interplay of viscosity and wettability controls fluid displacement in porous media, Phys. Rev. Fluids 8 (9) (9 2023), https://doi.org/10.1103/PhysRevFluids.8.094002.

[6] M. Trojer, M.L. Szulczewski, R. Juanes, Stabilizing fluid-fluid displacements in porous media through wettability alteration, Phys. Rev. Appl. 3 (5) (2015) 54008, https://doi.org/10.1103/PhysRevApplied.3.054008.

[7] K. Singh, M. Jung, M. Brinkmann, R. Seemann, Capillary-Dominated Fluid Displacement in Porous Media, 2018.

[8] M. Wang, Z. Wang, X. Gong, Z. Guo, The intensification technologies to water electrolysis for hydrogen production – a review, Renew. Sustain. Energy Rev. 29 (2014) 573–588, https://doi.org/10.1016/j.rser.2013.08.090.

[9] M.J. Blunt, Multiphase Flow in Permeable Media: A Pore-Scale Perspective, Cambridge University Press, Cambridge, 2017.

[10] S.M. Lößlein, R. Merz, D.W. Müller, M. Kopnarski, F. Mücklich, An in-depth evaluation of sample and measurement induced influences on static contact angle measurements, Sci. Rep. 12 (1) (2022) 19389, https://doi.org/10.1038/s41598-022-23341-3.

[11] T. Vukovic, J. Røstad, U. Farooq, O. Torsæter, A. van der Net, Systematic study of wettability alteration of glass surfaces by dichlorooctamethyltetrasiloxane silanization–a guide for contact angle modification, ACS Omega 8 (40) (2023) 36662–36676, https://doi.org/10.1021/acsomega.3c02448.

[12] L.E. Dalton, D. Tapriyal, D. Crandall, A. Goodman, F. Shi, F. Haeri, Contact angle measurements using sessile drop and micro-CT data from six sandstones, Transp. Porous Media 133 (1) (2020) 71–83, https://doi.org/10.1007/s11242-020-01415-y.

[13] J. Tudek, D. Crandall, S. Fuchs, C.J. Werth, A.J. Valocchi, Y. Chen, A. Goodman, In situ contact angle measurements of liquid CO2, brine, and Mount Simon sandstone core using micro X-ray CT imaging, sessile drop, and Lattice Boltzmann modeling, J. Pet. Sci. Eng. 155 (2017) 3–10, https://doi.org/10.1016/j.petrol.2017.01.047.

[14] R.T. Armstrong, C. Sun, P. Mostaghimi, S. Berg, M. Rücker, P. Luckham, A. Georgiadis, J.E. McClure, Multiscale characterization of wettability in porous media, Transp. Porous Media 140 (1) (2021) 215–240, https://doi.org/10.1007/s11242-021-01615-0.

[15] J. Schmatz, J.L. Urai, S. Berg, H. Ott, Nanoscale imaging of pore-scale fluid-fluid-solid contacts in sandstone, Geophys. Res. Lett. 42 (7) (2015) 2189–2195, https://doi.org/10.1002/2015GL063354.

[16] M. Vuckovac, M. Latikka, K. Liu, T. Huhtamäki, R.H.A. Ras, Uncertainties in contact angle goniometry, Soft Matter 15 (35) (2019) 7089–7096, https://doi.org/10.1039/C9SM01221D.

[17] C.H. Kung, P.K. Sow, B. Zahiri, W. Mérida, Assessment and interpretation of surface wettability based on sessile droplet contact angle measurement: challenges and opportunities, Adv. Mater. Interfaces 6 (18) (2019) 1900839, https://doi.org/10.1002/admi.201900839.

[18] T.T. Chau, A review of techniques for measurement of contact angles and their applicability on mineral surfaces, Miner. Eng. 22 (3) (2009) 213–219, https://doi.org/10.1016/j.mineng.2008.07.009.

[19] B. Charmas, R. Leboda, Effect of surface heterogeneity on adsorption on solid surfaces Application of inverse gas chromatography in the studies of energetic heterogeneity of adsorbents, Tech. rep., 2000, URL www.elsevier.com/locate/chroma.

[20] S. Mohammadi-Jam, K.E. Waters, Inverse gas chromatography applications: a review, Adv. Colloid Interface Sci. 212 (2014) 21–44, https://doi.org/10.1016/j.cis.2014.07.002.

[21] F. Thielmann, Introduction into the characterisation of porous materials by inverse gas chromatography, J. Chromatogr. A 1037 (1) (2004) 115–123, https://doi.org/10.1016/j.chroma.2004.03.060.

[22] A. Voelkel, B. Strzemiecka, K. Adamska, K. Milczewska, Inverse gas chromatography as a source of physiochemical data, J. Chromatogr. A 1216 (10) (2009) 1551–1566, https://doi.org/10.1016/j.chroma.2008.10.096.

[23] R. Ho, J.Y.Y. Heng, A review of inverse gas chromatography and its development as a tool to characterize anisotropic surface properties of pharmaceutical solids, KONA Powder Part. J. 30 (2013) 164–180, https://doi.org/10.14356/kona.2013016.

[24] O. Carrier, D. Bonn, Chapter 2 - Contact angles and the surface free energy of solids, in: D. Brutin (Ed.), Droplet Wetting and Evaporation, Academic Press, Oxford, 2015, pp. 15–23.

[25] B. Zhang, J. Wang, Z. Liu, X. Zhang, Beyond Cassie equation: local structure of heterogeneous surfaces determines the contact angles of microdroplets, Sci. Rep. 4 (1) (2014) 5822, https://doi.org/10.1038/srep05822.

[26] F. Thielmann, D. Pearse, Determination of surface heterogeneity profiles on graphite by finite concentration inverse gas chromatography, J. Chromatogr. A 969 (1) (2002) 323–327, https://doi.org/10.1016/S0021-9673(02)00896-8.

[27] R. Ho, A.S. Muresan, G.A. Hebbink, J.Y.Y. Heng, Influence of fines on the surface energy heterogeneity of lactose for pulmonary drug delivery, Int. J. Pharm. 388 (1) (2010) 88–94, https://doi.org/10.1016/j.ijpharm.2009.12.037.

[28] O. Planinšek, A. Trojak, S. Srčič, The dispersive component of the surface free energy of powders assessed using inverse gas chromatography and contact angle measurements, Int. J. Pharm. 221 (1) (2001) 211–217, https://doi.org/10.1016/S0378-5173(01)00687-1.

[29] J.W. Dove, G. Buckton, C. Doherty, A comparison of two contact angle measurement methods and inverse gas chromatography to assess the surface energies of theophylline and caffeine, Int. J. Pharm. 138 (2) (1996) 199–206, https://doi.org/10.1016/0378-5173(96)04535-8.

[30] R. Ho, S.J. Hinder, J.F. Watts, S.E. Dilworth, D.R. Williams, J.Y.Y. Heng, Determination of surface heterogeneity of d-mannitol by sessile drop contact angle and finite concentration inverse gas chromatography, Int. J. Pharm. 387 (1) (2010) 79–86, https://doi.org/10.1016/j.ijpharm.2009.12.011.

[31] N. Ahfat, G. Buckton, R. Burrows, M.D. Ticehurst, An exploration of interrelationships between contact angle, inverse phase gas chromatography and triboelectric charging data, Eur. J. Pharm. Sci. 9 (3) (2000) 271–276, https://doi.org/10.1016/S0928-0987(99)00063-9.

[32] M. Khodakarami, L. Alagha, D.J. Burnett, Probing surface characteristics of rare Earth minerals using contact angle measurements, atomic force microscopy, and inverse gas chromatography, ACS Omega 4 (8) (2019) 13319–13329, https://doi.org/10.1021/acsomega.9b01491.

[33] J.Y.Y. Heng, F. Thielmann, D.R. Williams, The effects of milling on the surface properties of form I paracetamol crystals, Pharm. Res. 23 (8) (2006) 1918–1927, https://doi.org/10.1007/s11095-006-9042-1.

[34] Y. Matsushita, S. Wada, K. Fukushima, S. Yasuda, Surface characteristics of phenol–formaldehyde–lignin resin determined by contact angle measurement and inverse gas chromatography, Ind. Crop. Prod. 23 (2) (2006) 115–121, https://doi.org/10.1016/j.indcrop.2005.04.004.

[35] G.L. Klein, G. Pierre, M.N. Bellon-Fontaine, M. Graber, Inverse gas chromatography with film cell unit: an attractive alternative method to characterize surface properties of thin films, J. Chromatogr. Sci. 53 (8) (2015) 1233–1238, https://doi.org/10.1093/chromsci/bmv008.

[36] M. Andrew, B. Bijeljic, M.J. Blunt, Pore-scale contact angle measurements at reservoir conditions using X-ray microtomography, Adv. Water Resour. 68 (2014) 24–31, https://doi.org/10.1016/j.advwatres.2014.02.014.

[37] J. Murison, B. Semin, J.-C. Baret, S. Herminghaus, M. Schröter, M. Brinkmann, Wetting heterogeneities in porous media control flow dissipation, Phys. Rev. Appl. 2 (3) (2014) 34002, https://doi.org/10.1103/PhysRevApplied.2.034002.

[38] J. Schultz, L. Lavielle, C. Martin, The role of the interface in carbon fibre-epoxy composites, J. Adhes. 23 (1) (1987) 45–60, https://doi.org/10.1080/00218468708080469.
[39] G.M. Dorris, D.G. Gray, Adsorption of n-alkanes at zero surface coverage on cellulose paper and wood fibers, J. Colloid Interface Sci. 77 (2) (1980) 353–362, https://doi.org/10.1016/0021-9797(80)90304-5.
[40] C.J. Van Oss, R.J. Good, M.K. Chaudhury, Additive and nonadditive surface tension components and the interpretation of contact angles, Langmuir 4 (4) (1988) 884–891, https://doi.org/10.1021/la00082a018.
[41] D.K. Owens, R.C. Wendt, Estimation of the surface free energy of polymers, J. Appl. Polym. Sci. 13 (8) (1969) 1741–1747, https://doi.org/10.1002/app.1969.070130815.
[42] F.M. Fowkes, Attractive forces at interfaces, Ind. Eng. Chem. 56 (12) (1964) 40–52, https://doi.org/10.1021/ie50660a008.
[43] L.-H. Lee, Roles of molecular interactions in adhesion, adsorption, contact angle and wettability, J. Adhes. Sci. Technol. 7 (6) (1993) 583–634, https://doi.org/10.1163/156856193X00871.
[44] A. van Asten, N. van Veenendaal, S. Koster, Surface characterization of industrial fibers with inverse gas chromatography, J. Chromatogr. A 888 (1) (2000) 175–196, https://doi.org/10.1016/S0021-9673(00)00487-8.
[45] G. Buckton, H. Gill, The importance of surface energetics of powders for drug delivery and the establishment of inverse gas chromatography, Adv. Drug Deliv. Rev. 59 (14) (2007) 1474–1479, https://doi.org/10.1016/j.addr.2007.06.017.
[46] H.E. Newell, G. Buckton, Inverse gas chromatography: investigating whether the technique preferentially probes high energy sites for mixtures of crystalline and amorphous lactose, Pharm. Res. 21 (8) (2004) 1440–1444, https://doi.org/10.1023/B:PHAM.0000036918.79205.4b.
[47] F. Thielmann, D.J. Burnett, J.Y.Y. Heng, Determination of the surface energy distributions of different processed lactose, Drug Dev. Ind. Pharm. 33 (11) (2007) 1240–1253, https://doi.org/10.1080/03639040701378035.
[48] A. Alghunaim, S. Kirdponpattara, B.-m.Z. Newby, Techniques for determining contact angle and wettability of powders, Powder Technol. 287 (2016) 201–215, https://doi.org/10.1016/j.powtec.2015.10.002.
[49] N. Otsu, A threshold selection method from gray-level histograms, IEEE Trans. Syst. Man Cybern. 9 (1) (1979) 62–66, https://doi.org/10.1109/TSMC.1979.4310076.
[50] A. AlRatrout, A.Q. Raeini, B. Bijeljic, M.J. Blunt, Automatic measurement of contact angle in pore-space images, Adv. Water Resour. 109 (2017) 158–169, https://doi.org/10.1016/j.advwatres.2017.07.018.
[51] D.H. Kaelble, Dispersion-polar surface tension properties of organic solids, J. Adhes. 2 (2) (1970) 66–81, https://doi.org/10.1080/0021846708544582.
[52] E. Chibowski, R. Perea-Carpio, Problems of contact angle and solid surface free energy determination, Adv. Colloid Interface Sci. 98 (2) (2002) 245–264, https://doi.org/10.1016/S0001-8686(01)00097-5.
[53] F. Ahmed, M. Zain-ul abdein, I.A. Channa, M.K. Yaseen, S.J. Gilani, M.A. Makhdoom, M. Mansoor, U. Shahzad, M.N.b. Jumah, Effect of ultrasonic surface mechanical attrition treatment-induced nanograins on the mechanical properties and biocompatibility of pure titanium, Materials 15 (15) (2022), https://doi.org/10.3390/ma15155097.
[54] C. Volpe, S. Siboni, Some reflections on acid–base solid surface free energy theories, J. Colloid Interface Sci. 195 (1) (1997) 121–136, https://doi.org/10.1006/jcis.1997.5124.
[55] A. Seidel-Morgenstern, Fundamentals and general terminology, in: Preparative Chromatography, John Wiley & Sons, Ltd, 2020, pp. 9–48, Ch. 2.
[56] S. Comte, R. Calvet, J.A. Dodds, H. Balard, Surface properties of low specific surface powders using inverse gas chromatography, Powder Technol. 157 (1) (2005) 39–47, https://doi.org/10.1016/j.powtec.2005.05.029.
[57] L. Liu, S.J. Tan, T. Horikawa, D.D. Do, D. Nicholson, J. Liu, Water adsorption on carbon - a review, Adv. Colloid Interface Sci. 250 (2017) 64–78, https://doi.org/10.1016/j.cis.2017.10.002.
[58] X. Shi, Y. Lin, X. Chen, Development of sorbent materials for direct air capture of CO2, Mater. Res. Soc. Bull. 47 (4) (2022) 405–415, https://doi.org/10.1557/s43577-022-00320-7.
[59] T. Li, J. Wang, F. Wang, L. Zhang, Y. Jiang, H. Arandiyan, H. Li, The effect of surface wettability and coalescence dynamics in catalytic performance and catalyst preparation: a review, ChemCatChem 11 (6) (2019) 1576–1586, https://doi.org/10.1002/cctc.201801925.
[60] Y.M. Volfkovich, V.E. Sosenkin, V.S. Bagotsky, Structural and wetting properties of fuel cell components, J. Power Sources 195 (17) (2010) 5429–5441, https://doi.org/10.1016/j.jpowsour.2010.03.002.